

RESEARCH ARTICLE

# Sensitivity analysis revealing the effect of modulating ionic mechanisms on calcium dynamics in simulated human heart failure

Maria T. Mora, Jose M. Ferrero, Lucia Romero, Beatriz Trenor\*

Centro de Investigación e Innovación en Bioingeniería, Universitat Politècnica de València, Valencia, Spain

\* [btrenor@eln.upv.es](mailto:btrenor@eln.upv.es)



**OPEN ACCESS**

**Citation:** Mora MT, Ferrero JM, Romero L, Trenor B (2017) Sensitivity analysis revealing the effect of modulating ionic mechanisms on calcium dynamics in simulated human heart failure. PLoS ONE 12(11): e0187739. <https://doi.org/10.1371/journal.pone.0187739>

**Editor:** Laszlo Csernoch, University of Debrecen, HUNGARY

**Received:** May 25, 2017

**Accepted:** October 25, 2017

**Published:** November 8, 2017

**Copyright:** © 2017 Mora et al. This is an open access article distributed under the terms of the [Creative Commons Attribution License](https://creativecommons.org/licenses/by/4.0/), which permits unrestricted use, distribution, and reproduction in any medium, provided the original author and source are credited.

**Data Availability Statement:** All relevant data are within the paper and its Supporting Information files.

**Funding:** This work was partially supported by the "Plan Estatal de Investigación Científica y Técnica y de Innovación 2013-2016" from the Ministerio de Economía, Industria y Competitividad of Spain and Fondo Europeo de Desarrollo Regional (FEDER) DPI2016-75799-R (AEI/FEDER, UE), and by Ministerio de Economía y Competitividad and Fondo Europeo de Desarrollo Regional (FEDER)

## Abstract

Abnormal intracellular  $\text{Ca}^{2+}$  handling is the major contributor to the depressed cardiac contractility observed in heart failure. The electrophysiological remodeling associated with this pathology alters both the action potential and the  $\text{Ca}^{2+}$  dynamics, leading to a defective excitation-contraction coupling that ends in mechanical dysfunction. The importance of maintaining a correct intracellular  $\text{Ca}^{2+}$  concentration requires a better understanding of its regulation by ionic mechanisms. To study the electrical activity and ionic homeostasis of failing myocytes, a modified version of the O'Hara et al. human action potential model was used, including electrophysiological remodeling. The impact of the main ionic transport mechanisms was analyzed using single-parameter sensitivity analyses, the first of which explored the modulation of electrophysiological characteristics related to  $\text{Ca}^{2+}$  exerted by the remodeled parameters. The second sensitivity analysis compared the potential consequences of modulating individual channel conductivities, as one of the main effects of potential drugs, on  $\text{Ca}^{2+}$  dynamic properties under both normal conditions and in heart failure. The first analysis revealed the important contribution of the sarcoplasmic reticulum  $\text{Ca}^{2+}$ -ATPase (SERCA) dysfunction to the altered  $\text{Ca}^{2+}$  homeostasis, with the  $\text{Na}^+/\text{Ca}^{2+}$  exchanger (NCX) and other  $\text{Ca}^{2+}$  cycling proteins also playing a significant role. Our results highlight the importance of improving the SR uptake function to increase  $\text{Ca}^{2+}$  content and restore  $\text{Ca}^{2+}$  homeostasis and contractility. The second sensitivity analysis highlights the different response of the failing myocyte versus the healthy myocyte to potential pharmacological actions on single channels. The result of modifying the conductances of the remodeled proteins such as SERCA and NCX in heart failure has less impact on  $\text{Ca}^{2+}$  modulation. These differences should be taken into account when designing drug therapies.

## Introduction

Heart failure (HF), characterized by contractile dysfunction and arrhythmogenesis, is the final stage of many cardiovascular diseases. To understand the mechanisms that lead to these pathological conditions, a large body of research has focused on the electrophysiological changes in failing myocytes. At the cellular level, the hallmarks of HF are a prolongation of the action

DPI2015-69125-R (MINECO/FEDER, UE). The funders had no role in study design, data collection and analysis, decision to publish, or preparation of the manuscript.

**Competing interests:** The authors have declared that no competing interests exist.

potential and alterations in ionic concentrations, such as intracellular  $\text{Na}^+$  ( $[\text{Na}^+]_i$ ) and  $\text{Ca}^{2+}$  ( $[\text{Ca}^{2+}]_i$ ), as a consequence of ion channel remodeling [1–4].

As intracellular  $\text{Ca}^{2+}$  is the main regulator of the cardiac excitation-contraction coupling, mishandling of  $\text{Ca}^{2+}$  is directly related to the mechanical dysfunction and certain arrhythmias associated with HF. Specifically, the alterations in  $\text{Ca}^{2+}$  dynamics are a decrease of the systolic peak, an increase of the diastolic level, a prolongation of the  $\text{Ca}^{2+}$  transient (CaT), and a reduced sarcoplasmic reticulum (SR)  $\text{Ca}^{2+}$  load [5–7], so that it is clear that restoring normal  $\text{Ca}^{2+}$  cycling in HF could have beneficial therapeutic effects.

The study of the reduced mechanical performance in failing human myocytes has shown a strong correlation with depressed intracellular  $\text{Ca}^{2+}$  transients and it has also been related to altered mRNA levels of  $\text{Ca}^{2+}$ -handling proteins [8]. Changes in the expression or activity of  $\text{Ca}^{2+}$  transport proteins in failing human ventricular myocytes, reviewed elsewhere [9–13], highlight the significant alteration in proteins involved in  $\text{Ca}^{2+}$  removal from the cytosol, such as the sarcoplasmic reticulum  $\text{Ca}^{2+}$ -ATPase (SERCA) and the  $\text{Na}^+/\text{Ca}^{2+}$  exchanger (NCX), and the existence of an important impaired diastolic  $\text{Ca}^{2+}$  release from the SR. On this basis, therapies are now being designed to restore  $\text{Ca}^{2+}$  homeostasis by targeting  $\text{Ca}^{2+}$ -handling proteins [14,15]. Most of these consist of improving SR function by increasing SR  $\text{Ca}^{2+}$  uptake or preventing SR  $\text{Ca}^{2+}$  leak, although they have not been systematically explored. There are also other ionic transporters involved in the electrophysiology of the heart that have not been analyzed from this point of view.

Pharmacological agents interacting with specific ionic channels can improve the electrical and mechanical properties of the heart. In fact, many studies have focused on the pharmacological effects on the action potential, but less attention has been paid to the effects on  $\text{Ca}^{2+}$  dynamics. The need for a better understanding of the mechanisms in this complex electrophysiological system requires a systematic methodology. Mathematical models and computational simulations can help identify and explain interactions and effects that cannot be easily understood experimentally. In cardiac electrophysiology, studies using this approach have provided new findings on the ionic basis of arrhythmogenic processes [16,17], while electromechanical models have highlighted the need for a balanced  $\text{Ca}^{2+}$  handling mechanism to prevent cardiac dysfunction, since treatments targeting increased contractility alone are not sufficient [18].

The aim of this study is thus to analyze *in silico* the alterations of  $\text{Ca}^{2+}$  handling in failing human myocytes and to identify possible pharmacological targets that could restore them. The first sensitivity analysis, performed in a HF model, elucidates the main mechanisms responsible for the alterations of  $\text{Ca}^{2+}$  homeostasis in such pathological conditions. Secondly, the comparison of two sensitivity analyses, in normal and failing conditions, reveals differences between both models in the effect of ionic parameters on  $\text{Ca}^{2+}$  handling. These findings suggest that pharmacological treatments might not produce the same results in HF as in healthy myocytes, meaning that it may be necessary to adapt the treatment to the specific pathological situation.

## Methods

### Human action potential model

The most recent and complete human ventricular action potential (AP) model is that of O'Hara et al. (ORd) [19], which provides a detailed description of  $\text{Ca}^{2+}$  handling, allowing the analysis of electrophysiological characteristics related to  $\text{Ca}^{2+}$ . A modified version of this model was used to simulate the electrophysiological activity at the cellular level. The reason for not using the original ORd formulation is that in a 1D multicellular fiber, conduction velocity

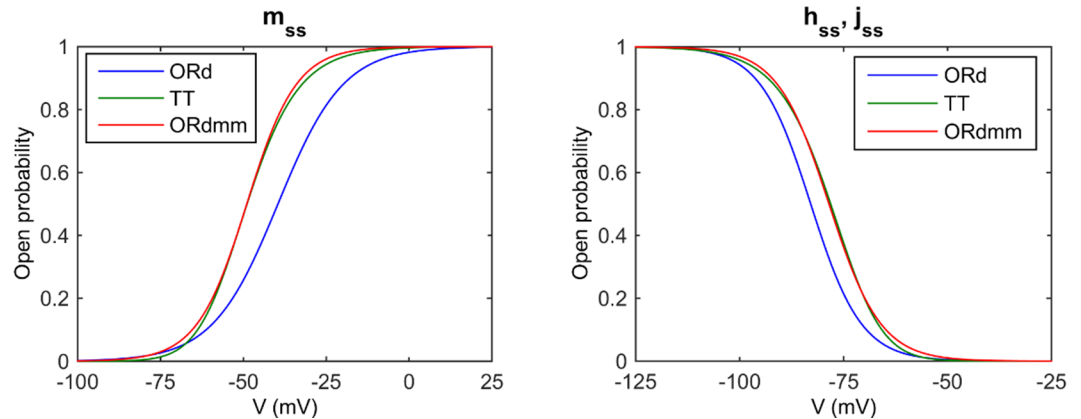


**Fig 1. Steady state activation (Left) and inactivation (Right) gates of the fast Na<sup>+</sup> current in the different models.** Original O’Hara et al. model (ORd), ten Tusscher et al. model (TT), and the modified ORd model (ORdmm).

<https://doi.org/10.1371/journal.pone.0187739.g001>

is low, especially under pathological situations when sodium current is reduced. Thus, the original fast sodium current ( $I_{Na}$ ) formulation was modified by shifting its steady state activation ( $m_{ss}$ ) and inactivation gates ( $h_{ss}$  and  $j_{ss}$ ), as depicted in Fig 1. Passini et al. [20] had already proposed an optimized formulation for the sodium steady-state inactivation response, which consisted basically of matching ten Tusscher et al. [21] curves by shifting the half potential and changing the slope. The  $m_{ss}$  was left-shifted, as suggested by Passini et al. [20], but we also modified the slope of the curve. The conductance ( $G_{Na}$ ) was reduced by 60% to maintain  $(dV/dt)_{max}$  in the range of 260 V/s.

Since it has been reported in voltage-clamp experiments [22] that the late sodium current ( $I_{NaL}$ ) is 0.07% of the value of  $I_{Na}$  peak at -30 mV after 200 ms, its conductance value ( $G_{NaL}$ ) was doubled to satisfy this condition. From now on, we will refer to the ORd modified model as the ORdmm.

## Simulation protocol

All the simulations in this study were carried out in endocardial cells paced at 1 Hz. Quantitative indicators characterizing  $Ca^{2+}$  dynamics were measured for the last of 1000 beats, after steady-state was reached (Figs 1 and 2 of the S1 File show the last traces of AP and CaT in different simulations). The measured electrophysiological (EP) indicators were: systolic peak and diastolic value of  $[Ca^{2+}]_i$ ,  $Ca^{2+}$  transient (CaT) duration measured as the time from upstroke to 30% and 80% recovery (CaTD<sub>30</sub> and CaTD<sub>80</sub>), rise time of CaT ( $t_{10-90}$ ) defined as the time from 10% CaT (close to the baseline) to 90% CaT (close to peak) (see Fig 2 for details). Other important concentrations are systolic and diastolic values of  $Ca^{2+}$  reached in the subspace ( $[Ca^{2+}]_{ss}$ ), representing the space near the T-tubules, and in the sarcoplasmic reticulum (SR), which is divided into the junctional (JSR) and network SR (NSR). AP duration (APD) was measured as the time from the upstroke to 30% and 90% repolarization (APD<sub>30</sub> and APD<sub>90</sub>), as well as the  $[Na^+]_i$  peak.

## Sensitivity analysis of the HF model

An AP model for the failing myocyte was formulated on the basis of experimental observations to reproduce the main EP characteristics under these conditions in failing human ventricular myocytes. Table 1 shows the changes performed in the ORdmm model, following Gomez et al.

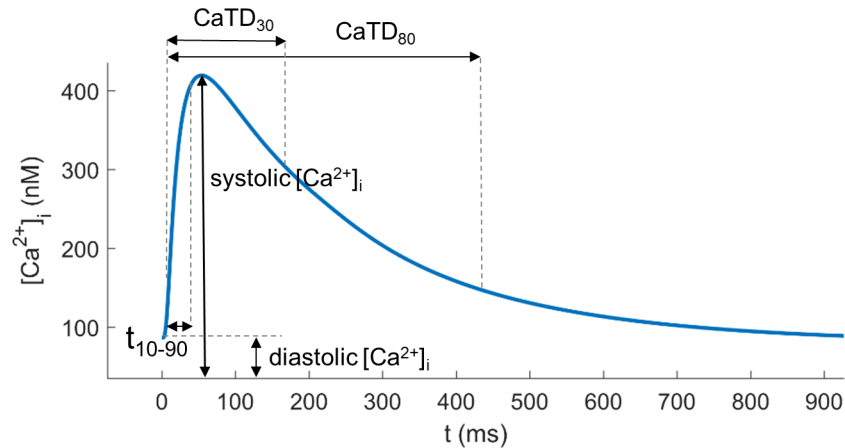


**Fig 2. Time course of a steady state  $\text{Ca}^{2+}$  transient (CaT) and its electrophysiological characteristics.** Systolic  $[\text{Ca}^{2+}]_i$  and diastolic  $[\text{Ca}^{2+}]_i$ , CaT duration measured as the time from upstroke to 30% and 80% recovery ( $\text{CaTD}_{30}$  and  $\text{CaTD}_{80}$ ) and 10% to 90% CaT rise time ( $t_{10-90}$ ).

<https://doi.org/10.1371/journal.pone.0187739.g002>

changes performed in the original ORd model [23]. This electrical remodeling consists of applying a scale factor to maximal conductances of the  $I_{\text{NaL}}$ , the transient outward  $\text{K}^+$  current ( $I_{\text{to}}$ ), and the inward rectifier  $\text{K}^+$  current ( $I_{\text{K1}}$ ), to the time constant of inactivation of the  $I_{\text{NaL}}$  ( $\tau_{\text{hL}}$ ), to the maximal fluxes of the  $\text{Na}^+/\text{K}^+$  ATPase current ( $I_{\text{NaK}}$ ), the  $\text{Na}^+/\text{Ca}^{2+}$  exchange current ( $I_{\text{NCX}}$ ), the  $\text{Ca}^{2+}$  uptake via SERCA pump ( $J_{\text{SERCA}}$ ), and the SR  $\text{Ca}^{2+}$  leak ( $J_{\text{leak}}$ ), to the fraction of active binding sites of the  $\text{Ca}^{2+}$  calmodulin-dependent protein kinase II (CaMKa), and to the SR  $\text{Ca}^{2+}$ -dependence of the steady-state activation of ryanodine receptor (RyR) release ( $K_{\text{rel,Ca}}$ ). Further details of these variables can be found in the Supplementary Material (S1 File).

A sensitivity analysis was performed to study the variability of HF remodeling. The ionic parameters altered in HF were varied one at a time with a new scale factor to assess the impact of their variability on  $\text{Ca}^{2+}$  dynamics. The baseline model was the ORdmm model with the EP

**Table 1. HF remodeling in ORdmm model.**

Ionic parameter	% in the HF model compared to the ORdmm
$I_{\text{NaL}}$	180%
$\tau_{\text{hL}}$	180%
$I_{\text{to}}$	40%
$I_{\text{K1}}$	68%
$I_{\text{NaK}}$	70%
$I_{\text{NCX}}$	175%
CaMKa	150%
$J_{\text{SERCA}}$	50%
$J_{\text{leak}}$	130%
$K_{\text{rel,Ca}}$	80%

The modified parameters are: the late  $\text{Na}^+$  current ( $I_{\text{NaL}}$ ), the time constant of inactivation of the  $I_{\text{NaL}}$  ( $\tau_{\text{hL}}$ ), the transient outward current ( $I_{\text{to}}$ ), the inward rectifier  $\text{K}^+$  current ( $I_{\text{K1}}$ ), the  $\text{Na}^+/\text{K}^+$  pump current ( $I_{\text{NaK}}$ ), the  $\text{Na}^+/\text{Ca}^{2+}$  exchanger ( $I_{\text{NCX}}$ ), the fraction of active binding sites of the  $\text{Ca}^{2+}$  calmodulin-dependent protein kinase II (CaMKa), the sarcoplasmic reticulum (SR)  $\text{Ca}^{2+}$  pump ( $J_{\text{SERCA}}$ ), the SR  $\text{Ca}^{2+}$  leak ( $J_{\text{leak}}$ ) and the sensitivity to  $[\text{Ca}^{2+}]_{\text{SR}}$  of the ryanodine receptors ( $\text{Ca}^{2+}$  sensitivity of  $J_{\text{rel},\infty}$ , called  $K_{\text{rel,Ca}}$ ).

<https://doi.org/10.1371/journal.pone.0187739.t001>

remodeling described in Table 1 (“HF basic”). Different degrees of HF were evaluated: without HF (“no change”), intermediate HF (“50% HF”) and severe HF (“150% HF”), and applied to one parameter at a time in each simulation, as detailed below. First, each remodeled variable was individually modified to its normal value as in the ORdmm model, i.e. without HF, while the others were fixed to the values of the basic HF model. This gave rise to 10 different “no change” models, each one for a specific parameter. The same parameters were similarly varied one at a time to a value representing  $\pm 50\%$  of that observed in the HF basic remodeling. In this way we obtained 10 different basic HF models in which only one parameter was at 50% of its HF condition (“50% HF”) and another 10 in which one parameter was increased by 50% of the basic HF remodeling (“150% HF”) (the exact percentages of change are specified in Table 1 in the S1 File). The different sensitivities of the most severe HF condition (“150% HF”) and the “no change” condition were then calculated, as described in Trenor et al. [17], where the indexes’ percentage of change ( $D_{c,p,x}$ ) and sensitivities ( $S_{c,p}$ ) were calculated as follows:

$$D_{c,p,x} = \frac{c_{p,x} - c_{basic}}{c_{basic}} \cdot 100 \tag{1}$$

$$S_{c,p} = \frac{D_{c,p,2} - D_{c,p,1}}{\Delta a} \tag{2}$$

with  $c_{p,x}$  being the magnitude of the characteristic “c” when parameter “p” undergoes a change with respect to the basic HF model ( $x = 1$ : without HF and  $x = 2$ : 150% HF), and  $c_{basic}$  the value of the same property in the basic HF model;  $\Delta a$  is the total interval of change of parameter p. The evaluated EP characteristics are the indicators specified in the simulation protocol section and were obtained from the steady-state APs and CaTs (see Figure A in S1 File). Finally, the calculated sensitivities were normalized to the maximum absolute sensitivity for each particular characteristic to facilitate the detection of the strongest effects.

### Sensitivity analysis of the effects of potential drugs

One of the aims of the present work is to study how potential drug-induced alterations in the main ionic currents could modulate important electrophysiological characteristics related to  $Ca^{2+}$  handling in normal and failing hearts. The methodology employed consisted of modulating individual ionic conductances or maximal fluxes by applying a scale factor of  $\pm 60\%$ . These variations were considered as a surrogate for enhancement or inhibition of one ionic transport mechanism due to the possible effect of a drug. The targeted currents or fluxes were the main parameters of the model, well known in the EP activity of myocytes:  $I_{Na}$ ,  $I_{NaL}$ ,  $I_{to}$ , the L-type  $Ca^{2+}$  current ( $I_{CaL}$ ), the rapid delayed rectifier  $K^+$  current ( $I_{Kr}$ ), the slow delayed rectifier  $K^+$  current ( $I_{Ks}$ ),  $I_{K1}$ ,  $I_{NCX}$ ,  $I_{NaK}$ ,  $J_{SERCA}$ , the SR  $Ca^{2+}$  release flux via RyR ( $J_{rel}$ ),  $J_{leak}$ , and the  $Na^+$  background current ( $I_{Nab}$ ). Since we wanted to study and compare the modulation in normal and failing conditions, these changes were applied to both models separately, obtaining two sensitivity analyses. When the HF model was used, modifications were done by maintaining the electrical remodeling affecting ionic parameters. Once the simulations had been performed, the EP characteristics were measured from the steady-state APs and CaTs (see Figure B in S1 File). For each EP characteristic and parameter, the indexes’ percentage of change ( $D_{c,p,x}$ ) and sensitivities ( $S_{c,p}$ ) were calculated similarly to those of the first sensitivity analysis (Eqs. 1 and 2). In this case, there were two basic models, the ORdmm model with and without HF, and sensitivities were calculated from the variation  $-60\%$  ( $x = 1$ ) to  $+60\%$  ( $x = 2$ );  $\Delta a$  remains constant and has a value of 1.2.

In the last step, to identify the parameters with the strongest influence on each EP indicator, the relative sensitivity was calculated as the ratio between each sensitivity and the maximum absolute sensitivity for that particular characteristic.

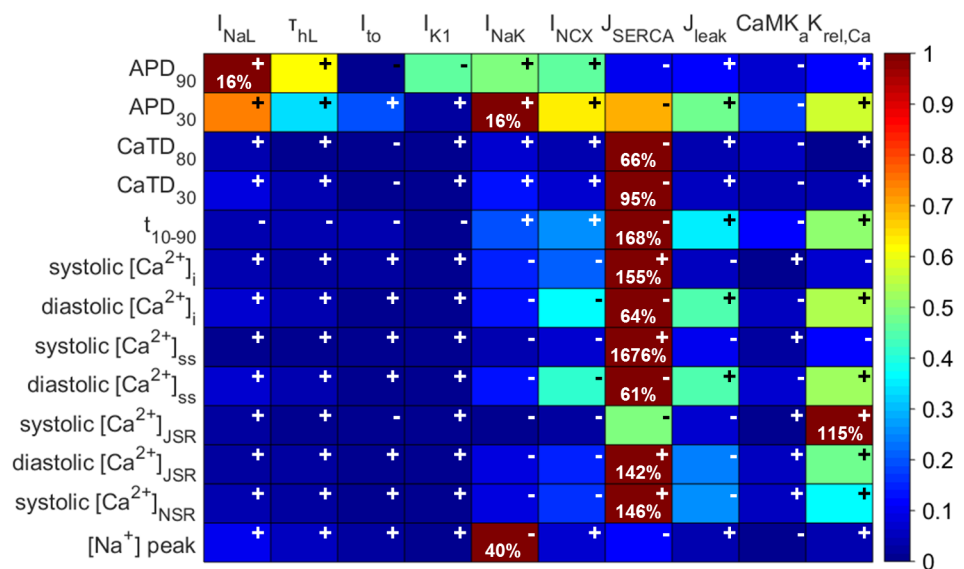
### Results

#### Impact of HF remodeling variability on Ca<sup>2+</sup> dynamics

Firstly, we analyzed the individual effects of the variability on the different ionic parameters remodeled in HF on Ca<sup>2+</sup> indicators (see Fig 3), to find the relative sensitivities of all the combinations of EP characteristics (vertical) to parameter variations (horizontal). A color scale, from dark blue to dark red highlights the strongest effects of each indicator (rows). The maximum absolute sensitivity (S<sub>c,p</sub>) is shown in each row to indicate the total impact of the parameters on a particular characteristic. In addition to sensitivity values, it is also important to find the dependency directions between the variables. For this, positive and negative signs indicate whether the change of the ionic current and the HF characteristic follow the same tendency or an inverse tendency, respectively.

From this sensitivity analysis, it can be deduced that I<sub>NaL</sub> and I<sub>NaK</sub> are the most important contributors to APD variations. The enhancement of both currents prolongs APD, but the former has a greater effect on APD<sub>90</sub> and the latter on APD<sub>30</sub>. τ<sub>hL</sub> and I<sub>NCX</sub> also have a mild effect.

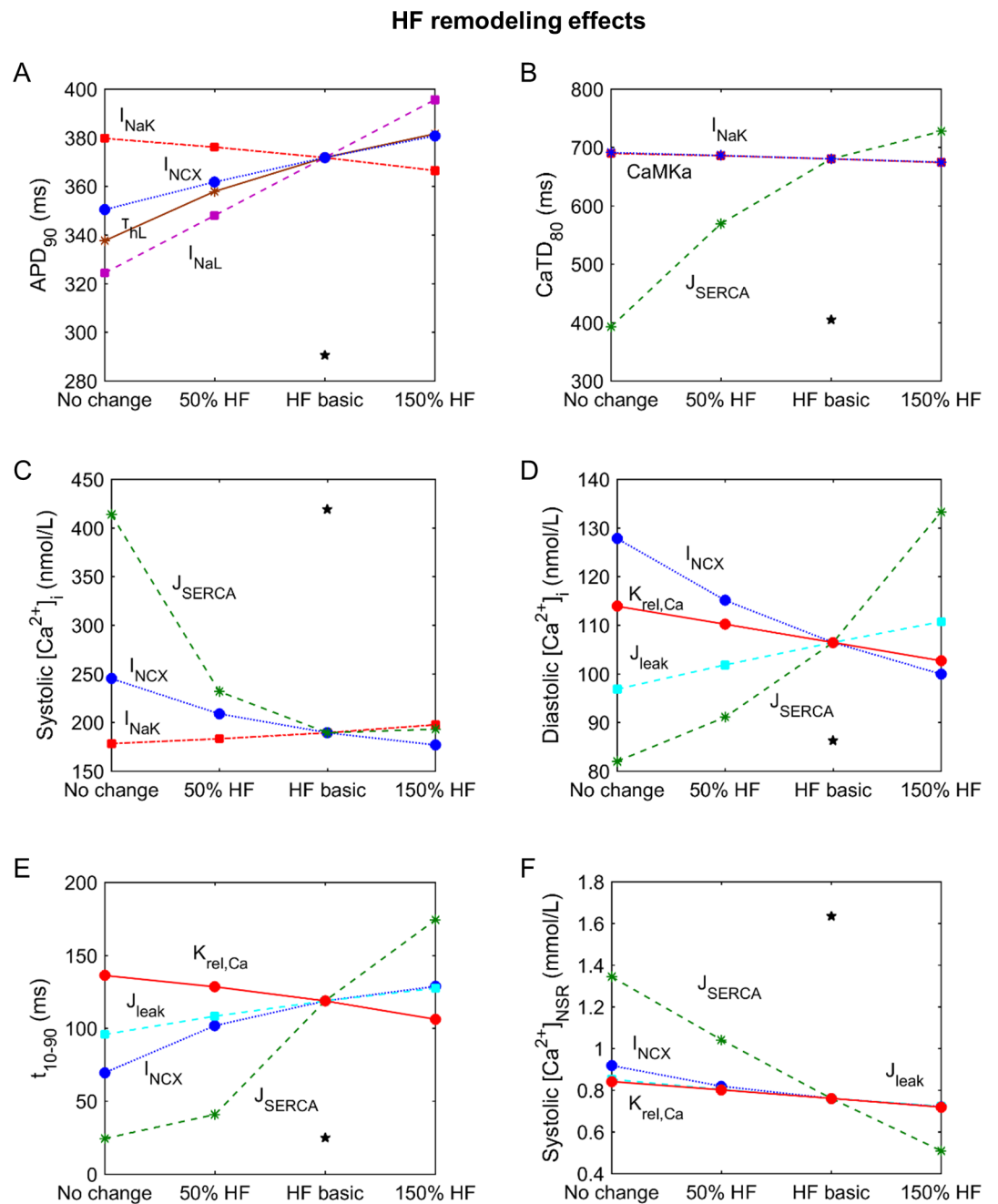
#### Sensitivity to HF remodeling



**Fig 3. Relative sensitivities of the electrophysiological properties to changes in electrophysiological remodeling in the HF model.** In the color scale, dark red indicates maximum relative sensitivity of a particular electrophysiological property to one ionic parameter, whereas dark blue indicates lack of dependency. Signs indicate whether the dependency is direct (+) or inverse (-). Percentages in each box indicate the maximum absolute sensitivity of the EP property in that row to one of the ionic parameters. The modulated parameters are: the late Na<sup>+</sup> current (I<sub>NaL</sub>), the time constant of inactivation of the I<sub>NaL</sub> (τ<sub>hL</sub>), the transient outward current (I<sub>to</sub>), the inward rectifier K<sup>+</sup> current (I<sub>K1</sub>), the Na<sup>+</sup>/K<sup>+</sup> pump current (I<sub>NaK</sub>), the Na<sup>+</sup>/Ca<sup>2+</sup> exchanger (I<sub>NCX</sub>), the fraction of active binding sites of the Ca<sup>2+</sup> calmodulin-dependent protein kinase II (CaMK<sub>a</sub>), the sarcoplasmic reticulum (SR) Ca<sup>2+</sup> pump (J<sub>SERCA</sub>), the SR Ca<sup>2+</sup> leak (J<sub>leak</sub>) and the sensitivity to [Ca<sup>2+</sup>]<sub>JSR</sub> of the RyR (Ca<sup>2+</sup> sensitivity of J<sub>rel,∞</sub>, called K<sub>rel,Ca</sub>). The electrophysiological properties are: action potential duration (APD<sub>90</sub> and APD<sub>30</sub>), Ca<sup>2+</sup> transient duration (CaTD<sub>80</sub> and CaTD<sub>30</sub>), rise time of CaT (t<sub>10-90</sub>), systolic and diastolic Ca<sup>2+</sup> levels in the cytosol ([Ca<sup>2+</sup>]<sub>i</sub>), the subsarcolemmal space ([Ca<sup>2+</sup>]<sub>ss</sub>), the junctional SR ([Ca<sup>2+</sup>]<sub>JSR</sub>) and the network SR ([Ca<sup>2+</sup>]<sub>NSR</sub>), and intracellular Na<sup>+</sup> peak ([Na<sup>+</sup>]<sub>i</sub>).

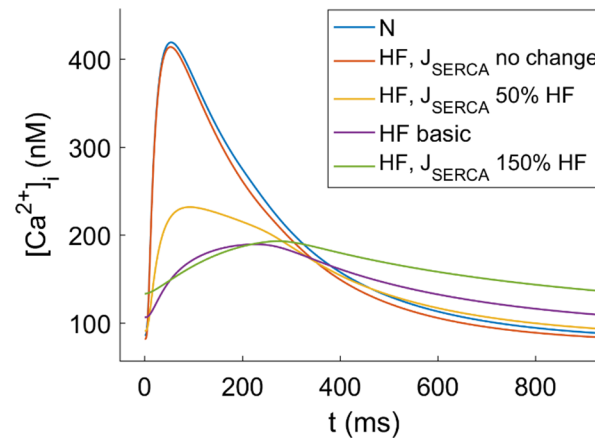
<https://doi.org/10.1371/journal.pone.0187739.g003>

Fig 4 shows the values of selected EP indicators with the variations of the parameters and the currents that exert a relevant influence. Panel A shows how APD<sub>90</sub> is modulated by these parameters.



**Fig 4. Sensitivity of electrophysiological properties to changes in ionic current parameters in the HF model.** Changes in APD<sub>90</sub> (panel A), CaTD<sub>80</sub> (panel B), systolic and diastolic  $[Ca^{2+}]_i$  (panels C and D), rise time of CaT (panel E) and SR  $Ca^{2+}$  systolic load (panel F) with the ionic parameters labeled. Axis x represents the simulation conditions; for “HF basic” the remodeling of the basic HF model is considered, for “No change” the labeled parameter is unchanged as it is in the ORdmm model, for “50% HF” the HF condition is reduced by 50% in the labeled parameter and for “150% HF” the HF condition is increased by 50%. The star represents the value of the indicator under simulated normal conditions.

<https://doi.org/10.1371/journal.pone.0187739.g004>



**Fig 5. Effect of  $J_{SERCA}$  remodeling in HF on CaTs.** Normal (N) vs failing (HF) conditions varying  $J_{SERCA}$  from the original value in the ORdmm model (no change) to 150% of its value in HF.

<https://doi.org/10.1371/journal.pone.0187739.g005>

Interestingly,  $J_{SERCA}$  is the major contributor to most of the EP properties related to  $Ca^{2+}$  dynamics (Fig 3). It can be seen in Fig 4 that the SERCA “no change” condition is able to restore these indicators to their normal values, despite EP remodeling in other parameters due to HF. Fig 5 shows the changes in CaT morphology due to SERCA remodeling in HF; a considerable recovery can be obtained by simply restoring the SR  $Ca^{2+}$  uptake function. CaTD shows a negative sensitivity to SERCA and the duration is increased with the inhibition of the pump during HF (Fig 4B, dashed green line). The other ionic parameters with an effect on CaTD are far from the influence of  $J_{SERCA}$ . For instance, although the reduction of  $I_{NaK}$  (dashed red line) has a positive dependence and could help to reduce the duration, the sensitivity value is small. Thus, restoring  $J_{SERCA}$  to its normal value would restore the CaTD value of non-failing myocytes (around 400 ms). The CaTD<sub>30</sub> sensitivities show a similar tendency to the CaTD<sub>80</sub> sensitivities in all the parameters but the values are higher.

Another important characteristic of  $Ca^{2+}$  dynamics is the rise time ( $t_{10-90}$ ). The SERCA pump is the strongest modulator of  $t_{10-90}$ . As shown in Fig 3,  $J_{leak}$  and  $K_{rel,Ca}$  also affect  $t_{10-90}$ , although to a lesser extent than SERCA. Both parameters are related with  $Ca^{2+}$  extrusion from the SR, in the cytosol and the subspace, respectively. Indeed  $K_{rel,Ca}$  is the sensitivity of  $J_{rel}$  to  $[Ca^{2+}]_{SR}$ , meaning that a reduction of  $K_{rel,Ca}$  leads to a higher release through RyRs. In general, HF conditions slow down the CaT rise, but reduced  $K_{rel,Ca}$  helps to accelerate it (Fig 4E, solid red line). The high impact of the abnormal SERCA function, increasing  $t_{10-90}$ , is one of the major problems in HF, and the enhancement of  $I_{NCX}$  (dotted blue line) contributes to a slow rise in CaT, although to a lesser extent.

$[Ca^{2+}]$  in all cell compartments is strongly modulated by the reduced  $J_{SERCA}$  in HF. Specifically, systolic  $[Ca^{2+}]_i$  values decrease when SERCA activity is reduced (Fig 4C), while diastolic concentrations increase (Fig 4D). The influence of  $I_{NCX}$  (dotted blue line) enhancement is also important and contributes to a general reduction of  $[Ca^{2+}]_i$ . Reduced  $I_{NaK}$  (dashed red line) also leads to higher systolic  $Ca^{2+}$ . Diastolic values are also sensitive to changes in  $J_{leak}$  and  $K_{rel,Ca}$  (dashed blue and solid red lines, respectively). In the subspace, the sensitivity of  $[Ca^{2+}]$  to ionic parameters is similar to the sensitivity in the cytoplasm, but with higher sensitivity values of the systolic  $Ca^{2+}$  peak (see rows 8 and 9 in Fig 3).

As the SR  $Ca^{2+}$  load is altered in HF and contributes to CaT changes,  $Ca^{2+}$  concentrations during an AP in this compartment were also analyzed. Both the junction and the network compartments have similar sensitivities to EP remodeling changes. In fact,  $J_{SERCA}$  (dashed

green line) remains the most important factor in modulating SR  $\text{Ca}^{2+}$  load, followed by  $J_{\text{leak}}$ ,  $K_{\text{rel,Ca}}$ , and  $I_{\text{NCX}}$  (Fig 4F). Exceptionally, it can be seen that in the JSR,  $K_{\text{rel,Ca}}$  is the main parameter that affects systolic concentration, closely followed by  $J_{\text{SERCA}}$  (see row 10 in Fig 3). The negative effect of  $J_{\text{SERCA}}$  on systolic  $[\text{Ca}^{2+}]_{\text{JSR}}$  is because of the smaller gradient between intracellular and SR  $[\text{Ca}^{2+}]$ , leading to lower  $J_{\text{rel}}$ . Consequently, the systolic  $[\text{Ca}^{2+}]_{\text{JSR}}$  minimum peak is less marked and the value becomes more positive as SERCA activity decreases.

The  $[\text{Na}^+]_i$  analysis shows high dependence on  $I_{\text{NaK}}$  in an inverse mode, as expected (Fig 3, last row), while the sensitivity of the rest of the parameters is less than 10%.

## Sensitivity of the normal and the HF model to potential effects of drugs

Fig 6 summarizes the results of the sensitivity analyses of AP and  $\text{Ca}^{2+}$  indicators to the same ionic modulation, simulating potential effects of pharmacological treatments in normal and failing conditions, showing the relative sensitivities on a color scale. The differences between the two models are indicated by the colors as well as by the different maximal sensitivities.

The response of normal and failing EP properties to the same changes in the main ionic currents can be seen in this sensitivity analysis. In general, the effects on EP characteristics follow the same tendency in both models, but with different sensitivities in some cases, showing a different response to the same change. Figs 7 and 8 show the most important ionic factors leading to important changes in the different indicators ( $\text{APD}_{90}$ ,  $\text{APD}_{30}$  and  $\text{CaTD}_{80}$  in Fig 7, and  $t_{10-90}$  and systolic and diastolic  $[\text{Ca}^{2+}]_i$  in Fig 8) in normal and failing myocytes.

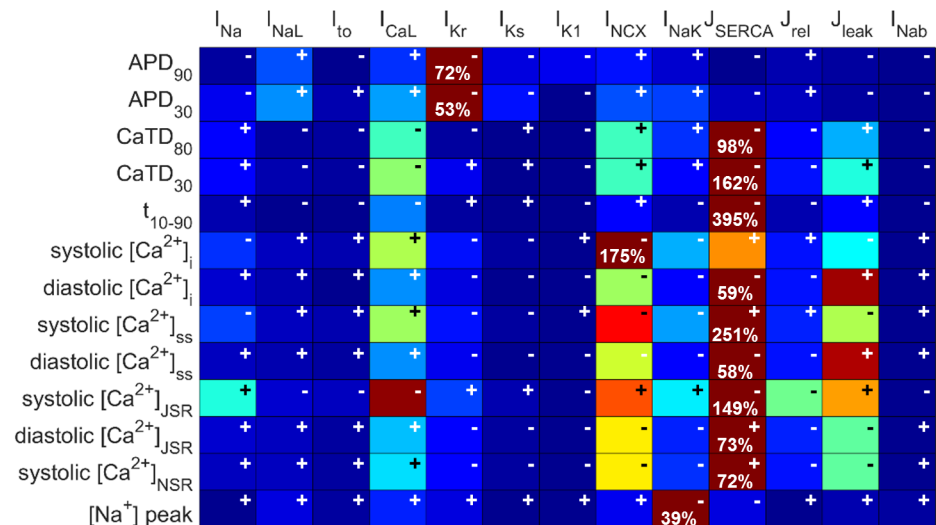
First, APD is highly sensitive to  $I_{\text{Kr}}$ , which shortens APD when the current is enhanced (Fig 6, rows 1 and 2 of both panels).  $I_{\text{NaL}}$  and  $I_{\text{CaL}}$  are also important contributors to APD changes. However, in comparison with normal conditions, in HF  $\text{APD}_{90}$  is more sensitive to changes in  $I_{\text{NaL}}$  (compare panels A and B of Fig 7, dashed magenta line). Furthermore,  $\text{APD}_{30}$  shows a negative dependency on  $I_{\text{CaL}}$  (dashed brown line) and  $J_{\text{SERCA}}$  (dashed green line) when these are reduced, which is not seen in normal conditions (Fig 7, panels C and D). Thus, under HF conditions, the  $I_{\text{NaL}}$  block should be more effective in reducing  $\text{APD}_{90}$  than in normal conditions, and unexpectedly, an  $I_{\text{CaL}}$  block or a reduction in  $J_{\text{SERCA}}$  could have negative effects and increase  $\text{APD}_{30}$ .

With respect to CaT characteristics in normal conditions, again  $J_{\text{SERCA}}$  seems to be the major contributor (Fig 6, rows 3–7 of both panels). CaTD has a negative sensitivity to SERCA, and although in HF this ionic transport also has a strong effect, it is less marked than in normal conditions. It can be observed that increasing the  $J_{\text{SERCA}}$  block in the HF model barely increases CaTD, compared to the lengthening produced in normal conditions (Fig 7, panels E and F, dashed green line). However, the enhancement of  $\text{Ca}^{2+}$  uptake reduces CaTD similarly in both conditions. Blocking NCX (dotted blue line) shortens CaTD, but the influence of  $I_{\text{CaL}}$  (dashed brown line) is reduced in HF in such a way that an enhancement of this current does not improve CaTD. On the other hand, it is to be noted that the effect of changes in  $I_{\text{Kr}}$  on CaTD in the HF model becomes important (Fig 6, row 4, panel B).  $I_{\text{Kr}}$  (dotted red line) block in HF prolongs CaTD, whereas this effect is non-existent in normal conditions. Thus,  $I_{\text{Kr}}$  block in HF could have negative effects on CaTD, in addition to the prolongation of APD.

Regarding CaT rise time ( $t_{10-90}$ ), a  $J_{\text{SERCA}}$  block in normal conditions significantly increases this property, acting as the most influential parameter. On the other hand, when it is enhanced, a very slight reduction of  $t_{10-90}$  is observed (Fig 8A, dashed green line). However, in HF, SERCA enhancement significantly contributes to the reduction of  $t_{10-90}$ , reaching a value close to the normal rise time (Fig 8B). Similar reductions can be obtained with the  $I_{\text{NCX}}$  block (dotted blue line).  $I_{\text{CaL}}$  and  $J_{\text{leak}}$  also modulate the rise time, especially in HF.

### Comparison of N and HF sensitivities

#### A. N conditions



#### B. HF conditions

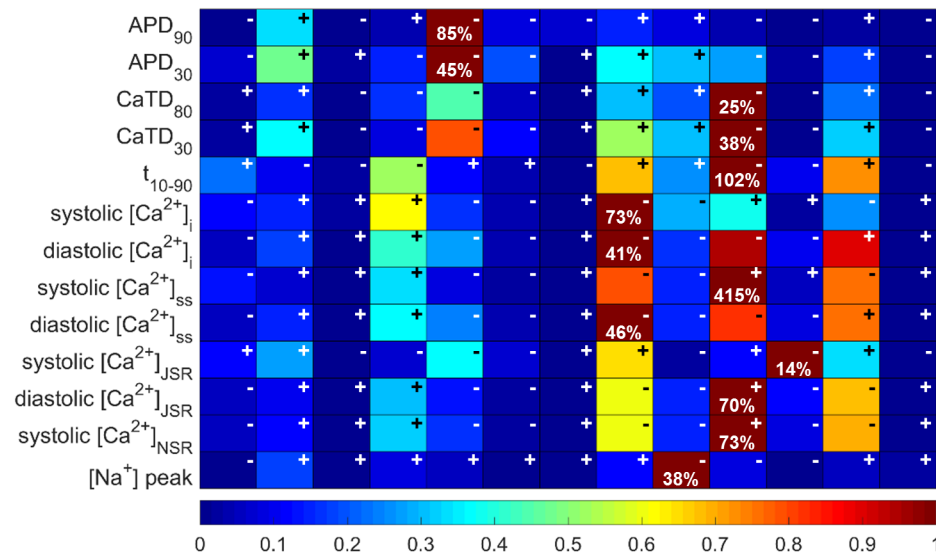


**Fig 6. Relative sensitivities of the electrophysiological properties to modulating effects of potential drugs. Sensitivities in normal (panel A) and failing conditions (panel B).** In the color scale, dark red indicates maximum relative sensitivity of a particular electrophysiological property to one ionic parameter, whereas dark blue indicates lack of dependency. Signs indicate whether the dependency is direct (+) or inverse (-). Percentages in each box indicate the maximum absolute sensitivity of the EP property in that row for all ionic parameters. The modulated parameters are: the fast  $Na^+$  current ( $I_{Na}$ ), the late  $Na^+$  current ( $I_{NaL}$ ), the transient outward  $K^+$  current ( $I_{to}$ ), the L-type  $Ca^{2+}$  current ( $I_{CaL}$ ), the rapid delayed rectifier  $K^+$  current ( $I_{Kr}$ ), the slow delayed rectifier  $K^+$  current ( $I_{Ks}$ ), the inward rectifier  $K^+$  current ( $I_{K1}$ ), the  $Na^+/Ca^{2+}$  exchange current ( $I_{NCX}$ ), the  $Na^+/K^+$  pump current ( $I_{NaK}$ ), the  $Ca^{2+}$  uptake via SERCA pump ( $J_{SERCA}$ ), the SR  $Ca^{2+}$  release flux via RyR ( $J_{rel}$ ), the SR  $Ca^{2+}$  leak ( $J_{leak}$ ) and the  $Na^+$  background current ( $I_{Nab}$ ). The electrophysiological properties are: action potential duration (APD<sub>90</sub> and APD<sub>30</sub>),  $Ca^{2+}$  transient duration (CaTD<sub>80</sub> and CaTD<sub>30</sub>), rise time of CaT ( $t_{10-90}$ ), systolic and diastolic  $Ca^{2+}$  levels in the cytosol ( $[Ca^{2+}]_i$ ), the subsarcolemmal space ( $[Ca^{2+}]_{ss}$ ), the junctional SR ( $[Ca^{2+}]_{JSR}$ ) and the network SR ( $[Ca^{2+}]_{NSR}$ ), and intracellular  $Na^+$  peak ( $[Na^+]_i$ ).

<https://doi.org/10.1371/journal.pone.0187739.g006>

Ionic modulation effects

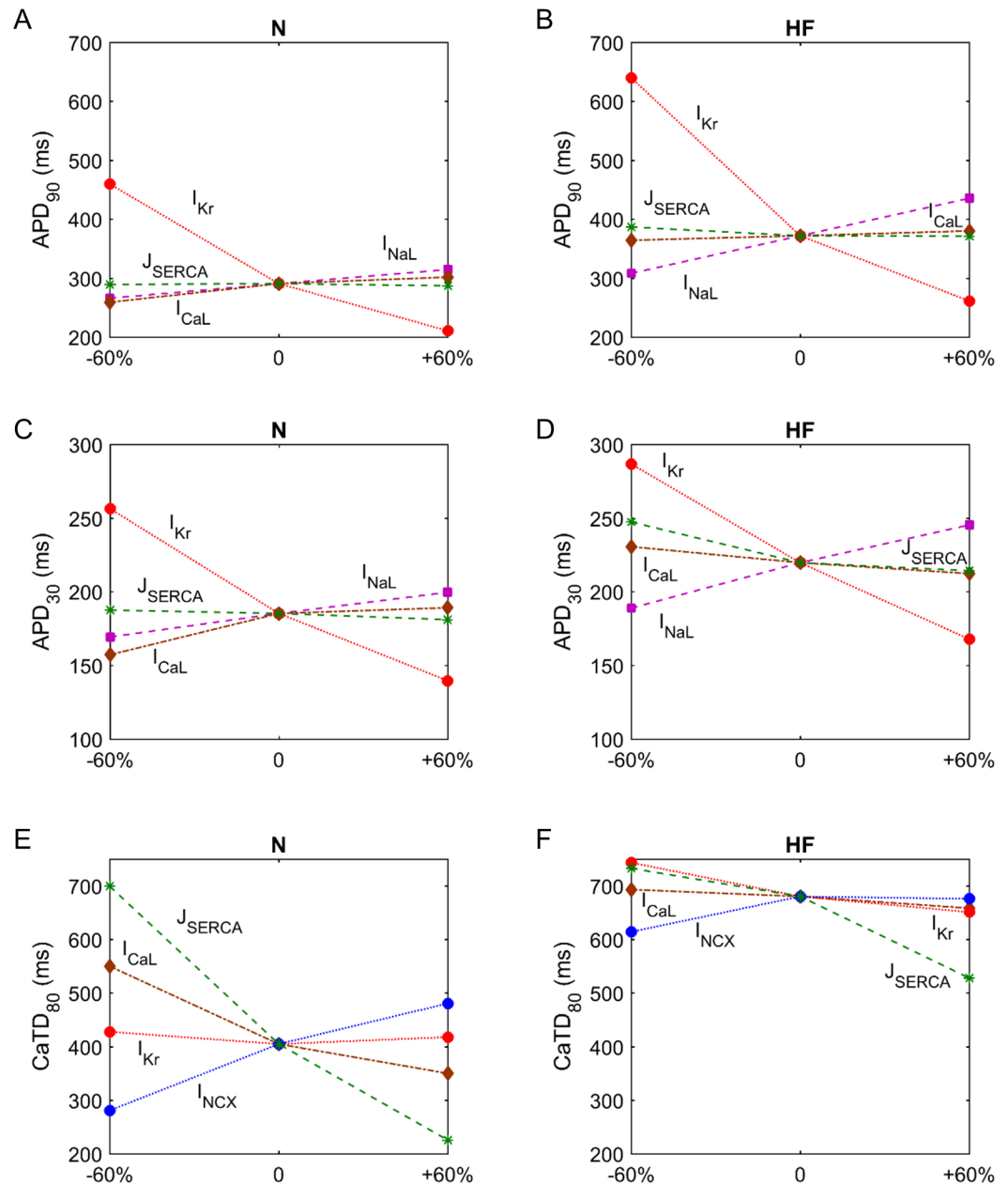


**Fig 7. Sensitivity of APD<sub>90</sub>, APD<sub>30</sub> and CaTD<sub>80</sub> to the effects of drugs in normal (N) and failing (HF) conditions.** Changes in APD<sub>90</sub> (panels A and B), APD<sub>30</sub> (panels C and D) and CaTD<sub>80</sub> (panels E and F). Axis x represents simulation conditions; for “0” the basic model is considered, for “± 60%” the labeled parameter has been changed by this percentage.

<https://doi.org/10.1371/journal.pone.0187739.g007>

[Ca<sup>2+</sup>] in all cell compartments is highly regulated by J<sub>SERCA</sub>, followed by I<sub>NCX</sub>, J<sub>leak</sub>, and I<sub>CaL</sub> (Fig 6, rows 6–12). J<sub>SERCA</sub> enhancement contributes to the increase of systolic levels and Ca<sup>2+</sup> SR load and to the reduction of diastolic levels. However, I<sub>NCX</sub> inhibition increases Ca<sup>2+</sup> concentration and has a greater effect than SERCA during systole (Fig 6, row 6). In HF, these parameters have less impact on the Ca<sup>2+</sup> peak and the modification of I<sub>NCX</sub> (dotted blue line)

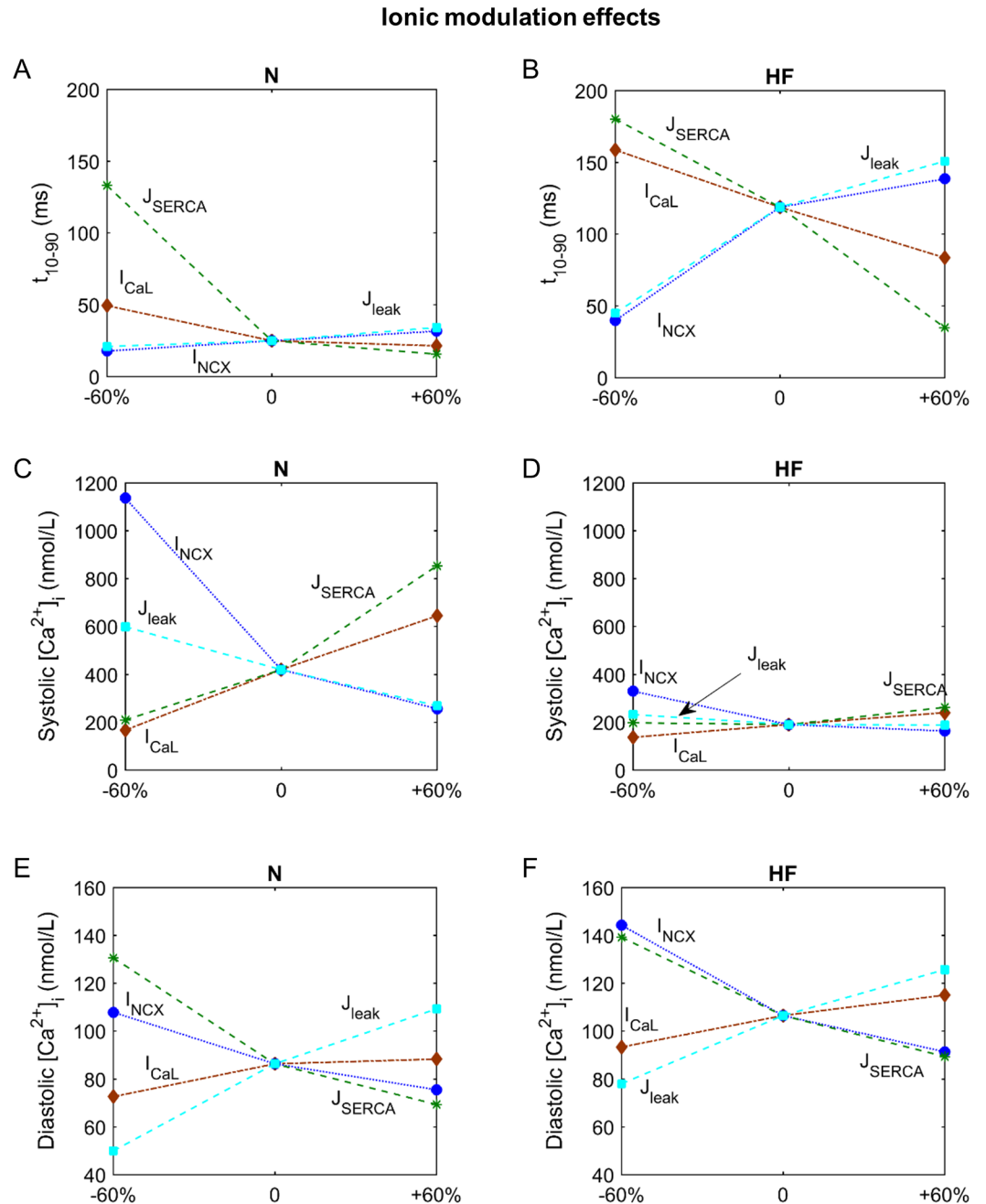


**Fig 8. Sensitivity of  $t_{10-90}$ , systolic and diastolic  $[Ca^{2+}]_i$  to the effects of drugs in normal (N) and failing (HF) conditions.** Changes in the rise time of CaT (panels A and B), in systolic and diastolic  $[Ca^{2+}]_i$  (panels C, D and E, F). Axis x represents simulation conditions; for “0” the basic model is considered, for “±60%” the labeled parameter has been changed by this percentage.

<https://doi.org/10.1371/journal.pone.0187739.g008>

and  $J_{SERCA}$  (dashed green line) produce smaller variations than those in normal conditions (Fig 8, panels C and D). Diastolic  $[Ca^{2+}]_i$  presents a similar sensitivity to  $I_{NCX}$  and  $J_{SERCA}$  in HF and normal conditions. However, the  $I_{NCX}$  block (dotted blue line) has a relevant effect, enhancing diastolic levels and worsening HF changes (Fig 8, panels E and F). In the subspace,

responses to variations in ionic currents are similar to those of the cytosol but with higher sensitivity values during the systole (Fig 6, rows 8 and 9).

$\text{Ca}^{2+}$  concentrations in the SR are also regulated by  $J_{\text{SERCA}}$ , followed by  $J_{\text{leak}}$  and  $I_{\text{NCX}}$ .  $J_{\text{rel}}$  seems to affect only systolic  $[\text{Ca}^{2+}]_{\text{SR}}$  in HF, whereas in normal conditions it is a secondary influence (Fig 6, rows 10–12).

Finally, the  $[\text{Na}^+]_i$  analysis shows high sensitivity to  $I_{\text{NaK}}$  in an inverse mode. There are no important differences between normal and HF sensitivities, but  $I_{\text{NaL}}$  has a higher impact in HF (Fig 6, last row).

## Discussion

### Major findings

In this study  $\text{Ca}^{2+}$  dynamics and APs were simulated in a human ventricular model (ORdmm) to shed light on the role of some ionic current characteristics and reveal other mechanisms that may take part in  $\text{Ca}^{2+}$  cycling during HF. The first sensitivity analysis highlights the strong effect of  $J_{\text{SERCA}}$ , among other parameters remodeled in HF, on the modulation of  $\text{Ca}^{2+}$  indicators. Under HF conditions, depressed SERCA activity worsens all the EP characteristics related to  $\text{Ca}^{2+}$ , which are the hallmark of HF: CaT rise time, systolic and diastolic  $[\text{Ca}^{2+}]$ , CaT duration and SR  $\text{Ca}^{2+}$  content. Enhancing the SERCA uptake function to its normal activity improves all these  $\text{Ca}^{2+}$  characteristics and could restore contraction.

The comparison of  $\text{Ca}^{2+}$  sensitivities to drug-induced alterations in the main ionic currents in normal and HF conditions reveals some parameters that modulate  $\text{Ca}^{2+}$  dynamics in a different way. As blocking  $I_{\text{Kr}}$  has a marked influence in prolonging CaTD in HF in comparison to its effect in normal conditions,  $I_{\text{Kr}}$  blocking drugs should be avoided in HF for their impact not only on APD but also on contractility. Blocking  $I_{\text{NCX}}$  could be beneficial in HF, as it improves CaT rise time, however it could also increase diastolic  $[\text{Ca}^{2+}]_i$ , which worsens contraction. These opposing effects should be taken into account when considering blocking NCX. SERCA enhancement in HF is highly effective in reducing  $t_{10-90}$ , but its depressed activity requires extreme enhancement to restore systolic  $[\text{Ca}^{2+}]_i$ .

### Comparison with experimental results

In this work the electrophysiological activity of human ventricular myocytes was simulated using the latest human AP model with a detailed formulation of  $\text{Ca}^{2+}$  dynamics [19], using  $\text{Ca}^{2+}$  cycling formulated from human experimental data. However, the simulated  $\text{Ca}^{2+}$  transients and concentrations are generally smaller than those found in the literature, possibly because of the high electrophysiological variability of the experimental data, due in part to the fluorescence-based technique used to measure intracellular  $\text{Ca}^{2+}$  [5,7,24]. Despite these drawbacks, simulations are able to mimic  $\text{Ca}^{2+}$  transients and reproduce the abnormalities in  $\text{Ca}^{2+}$  dynamics observed in failing human hearts. The main alterations are long  $\text{Ca}^{2+}$  transients of reduced amplitude and SR with less  $\text{Ca}^{2+}$  content [3,25,26].

Some experimental studies have focused on the main ionic transporters taking part in  $\text{Ca}^{2+}$  cycling (L-type  $\text{Ca}^{2+}$  channels, RyR channels, SERCA, and NCX) to improve contraction [14,15,27,28], and many mechanistic details of  $\text{Ca}^{2+}$  dynamics have been discovered to date. The present work was designed to analyze these mechanisms under different conditions (normal and heart failure) to complement the experimental results and increase our understanding of how they work. From our sensitivity analysis, it can be seen that SERCA plays an important role in modulating  $\text{Ca}^{2+}$ . SERCA's main function is to remove cytosolic  $\text{Ca}^{2+}$  and reintroduce it into the SR during diastole for myocardial relaxation. It is therefore reasonable to assume that reducing SERCA activity would increase diastolic  $[\text{Ca}^{2+}]_i$ , slow the rate of CaT decay, and

reduce the SR  $\text{Ca}^{2+}$  load. SR  $\text{Ca}^{2+}$  store depletion indirectly reduces  $\text{Ca}^{2+}$  release and systolic function. In fact, after  $\text{Ca}^{2+}$  uptake function inhibition, healthy myocytes showed changes in CaT and SR  $\text{Ca}^{2+}$  content, for example using the use of thapsigargin or TBQ in rats [29–31]. Under failing conditions, we obtained the same alterations in  $\text{Ca}^{2+}$  indicators, which presented a high sensitivity to SERCA, which highlights the strong effect of SERCA on the rest of the ionic mechanisms affected by HF remodeling. Increased inhibition of the SERCA function resulted in higher alteration in  $\text{Ca}^{2+}$  dynamics, while the restoration of a normal SR  $\text{Ca}^{2+}$  uptake showed a significant improvement of all these EP characteristics. Specific pharmacological agents to enhance SERCA activity have not been developed so far, but our results can be compared with those obtained using gene therapy methods. In agreement with our simulations of SERCA variability in normal conditions, transgenic rabbit cardiomyocytes overexpressing SERCA led to an increased magnitude of CaT and SR content compared to the control [32]. However, Morimoto et al. [33] did not find significant changes in SR  $\text{Ca}^{2+}$  content nor in time to peak in transgenic mice, although SERCA overexpression did increase the CaT peak, which could be related with the insignificant effect on  $t_{10-90}$  in normal conditions that we observed in our analysis with enhanced SERCA.

Enhancing SERCA in HF improves cellular  $\text{Ca}^{2+}$  homeostasis. SERCA overexpression in failing cells restored  $\text{Ca}^{2+}$  handling in rats [34], as well as in humans [35]. In our simulations, a 60% increase in SERCA activity led to the lower recovery of  $\text{Ca}^{2+}$  indicators in HF than in normal conditions. Indeed, the depressed activity of the pump in HF is responsible for these discrepancies, and studies should be performed taking into account that different results may be obtained applying the same therapy under normal and failing conditions. Rocchetti et al. [36] observed that istaroxime stimulated SERCA uptake function in failing myocytes, restoring  $\text{Ca}^{2+}$  levels and, in contrast to our results, the effect on failing myocytes was higher than on the non-failing ones. However, differences between experiments and simulations should be taken with caution. Our 60% SERCA enhancement represents an increase of the downregulated protein in HF whereas istaroxime seems to restore the abnormal SR  $\text{Ca}^{2+}$  uptake function by targeting secondary molecules interacting with the pump, such as PLB. There might be other sources for discrepancies between our simulation results and Rocchetti et al. experiments, such as species differences (guinea pig vs human myocytes), HF stage, and EP remodeling.

The altered NCX activity in HF also has an impact on  $\text{Ca}^{2+}$  handling. An increased reverse mode occurs due to  $[\text{Na}^+]_i$  accumulation, increasing  $\text{Ca}^{2+}$  influx. At the same time, the upregulated forward mode increases  $\text{Ca}^{2+}$  efflux, resulting in cellular  $\text{Ca}^{2+}$  loss and a reduced SR  $\text{Ca}^{2+}$  load. Therefore, most of the consequences of remodeled NCX worsen  $\text{Ca}^{2+}$  dynamics and the possible beneficial effect of NCX inhibition has been analyzed in several studies. SEA0400, a NCX inhibitor, did not produce significant changes either in the shape or in the magnitude of the CaT in normal guinea pig or canine myocytes [37–39], although Ozdemir et al. [40] observed an increased CaT peak and SR  $\text{Ca}^{2+}$  content in pigs. However, positive effects were also observed on  $\text{Ca}^{2+}$  homeostasis in transgenic animals with NCX overexpression [41,42], as observed in the present simulations. These results suggest a dependency on the animal model and highlight the need for human experimental data, as well as the careful selection of the pharmacological agent. SN-6, another NCX inhibitor, was found to have a negative inotropic action in normal and failing cardiomyocytes, with a greater reduction of SR  $\text{Ca}^{2+}$  content in HF [43]. In this case, the non-specificity of the blocker and the effect on other currents, such as  $I_{\text{CaL}}$  can affect the results, so that further experimental studies are required to clarify the effects of NCX inhibition, especially in the failing human myocardium.

The third pathway related to sarcoplasmic  $\text{Ca}^{2+}$  is its release through RyR channels. In HF, these  $\text{Ca}^{2+}$  proteins undergo a slightly increased  $\text{Ca}^{2+}$  sensitivity, which favors the  $\text{Ca}^{2+}$ -induced  $\text{Ca}^{2+}$  release process. The main problem in HF is that RyRs become leaky and  $\text{Ca}^{2+}$  is released

spontaneously during diastole, typically in the form of  $\text{Ca}^{2+}$  sparks [44]. As our HF model reproduces the effect of  $J_{\text{leak}}$ , contributing to abnormal  $\text{Ca}^{2+}$  cycling, its inhibition would thus be beneficial for myocardial contraction. However, in the ORd model,  $J_{\text{leak}}$  was formulated independently of the RyR channel, representing a continuous  $\text{Ca}^{2+}$  leakage from the SR through the SERCA pump. In this case, it is not possible to compare our results with the effects of any drug able to alleviate this leak. In our simulation study, sensitivity to RyR channels ( $J_{\text{rel}}$ ) was analyzed independently of  $J_{\text{leak}}$ . This ionic mechanism did not have strong effects on  $\text{Ca}^{2+}$  dynamics in our simulations, unlike most of the published experimental results. Inducing  $\text{Ca}^{2+}$ -leak with caffeine or ryanodine in rats reduced CaT amplitude and changed systolic and diastolic concentrations [30]. Tetracaine, an RyR inhibitor, could reverse these variations and restore normal  $\text{Ca}^{2+}$  dynamics. Since caffeine decreases SR  $\text{Ca}^{2+}$  content, increasing the activity of the RyR does not have a positive inotropic effect [45], but the negative effects are not clear.

## Benefits and predictions from systematic sensitivity analyses

Unlike experimental studies, sensitivity analyses are a systematic methodology that allows many parameters to be varied either independently (one at a time) or at the same time, which avoids the difficulty of replicating conditions and allows the control of all the sources of variability that affect experimental results. The selection of the animal species when analyzing cellular electrophysiology is one of the most influential factors. Due to the need for human data and the scarcity of human hearts for experimental purposes, the use of a detailed human model such as the ORd model is extremely useful. Modeling and simulation also allow the assessment of EP characteristics, which cannot be measured experimentally, such as  $[\text{Ca}^{2+}]$  in different cellular compartments. With this approach, the modification of each parameter is quantified, while this cannot always be done accurately in experiments.

The use of sensitivity analyses has been widely extended to study physiological processes providing valuable predictions [16,17]. Other commonly used methods are multivariate analyses, which can provide additional information to that obtained with single parameter analyses [46,47]. However, we chose the simplicity and intuitive interpretation of the results by changing parameters individually, as this is also an accepted method used in this type of study [16,17]. Once the consistency of the sensitivity analyses results have been verified and compared against available experimental data, predictions can be made of how specific EP indicators are modulated by changes in ionic parameters for which data are not available. In agreement with previous studies,  $I_{\text{Kr}}$  block and  $I_{\text{NaL}}$  enhancement prolong APD, a situation aggravated under failing conditions [48–50]. The high sensitivity of  $[\text{Na}^+]_i$  to  $I_{\text{NaK}}$  and the increase in  $[\text{Na}^+]_i$  due to the dysfunction of this pump in HF extruding less  $\text{Na}^+$  out of the cell were also as expected [51,52]. This  $[\text{Na}^+]_i$  accumulation is related to APD shortening when the electrogenic  $\text{Na}^+/\text{K}^+$  pump is inhibited because it increases the NCX reverse mode (outward current) and contributes to cell repolarization [16,17,51,53]. Other modulations of EP characteristics by ionic parameters in HF are less obvious. For instance, blocking  $I_{\text{CaL}}$  and  $J_{\text{SERCA}}$  may have negative prolonging effects on  $\text{APD}_{30}$  which does not occur under normal conditions. In terms of  $\text{Ca}^{2+}$  characteristics, blocking  $I_{\text{Kr}}$  prolongs CaTD. The present simulation results predict that several  $\text{Ca}^{2+}$  indicators are unexpectedly more influenced by changes in  $I_{\text{NCX}}$  than changes in SERCA in the failing myocyte. Unfortunately, the supposed beneficial blocking of NCX has negative consequences on diastolic  $[\text{Ca}^{2+}]_i$  (raising its value), while enhancing SERCA always contributes to improving  $\text{Ca}^{2+}$  dynamics. These predictions would of course need to be validated using experimental results. The strength of systematic sensitivity analyses is their predictive power and the indications they provide for the design of the required experiments thus contributing to reducing the time and costs involved in drug design.

## Limitations of the study

The limitations of the present study are linked, on the one hand, to the use of a mathematical model for the action potential. Despite its validation using human data, there are still some quantitative differences in intracellular  $\text{Ca}^{2+}$  levels. Additionally, in some situations, the model does not represent all the ionic mechanisms that are commonly described in the literature as is the case of  $J_{\text{leak}}$  which, in the ORD model, was formulated only as a backflux of the SERCA pump. However, in other models [21,54,55],  $J_{\text{leak}}$  is considered as a secondary efflux through the RyR channels, sometimes coexisting with a reverse SERCA flux [44]. For this reason, the analysis of the effects of  $J_{\text{leak}}$  and  $J_{\text{rel}}$  should be taken with caution, i.e. accordingly to the model formulation. Also, in our study,  $J_{\text{SERCA}}$  was considered separately from the  $J_{\text{leak}}$  term, both of them included in the original ORD  $J_{\text{up}}$  formulation. Finally, the electrical remodeling associated with HF is not unique [23,56–58], as there are discrepancies and variations regarding some ionic currents due to the data generated in different experimental studies.

The scarcity of available human data has hampered the validation of our results, thus affecting their predictive value, and the wide variations in the existing experimental studies on different species and treatments, also make the validation of the simulations difficult.

## Supporting information

**S1 File. Supplemental material.** Extended Methods and Steady-state conditions. (DOCX)

## Author Contributions

**Conceptualization:** Jose M. Ferrero, Beatriz Trenor.

**Data curation:** Maria T. Mora.

**Formal analysis:** Maria T. Mora.

**Funding acquisition:** Beatriz Trenor.

**Investigation:** Maria T. Mora.

**Methodology:** Maria T. Mora, Lucia Romero, Beatriz Trenor.

**Project administration:** Jose M. Ferrero, Beatriz Trenor.

**Software:** Maria T. Mora.

**Supervision:** Jose M. Ferrero, Beatriz Trenor.

**Visualization:** Maria T. Mora, Beatriz Trenor.

**Writing – original draft:** Maria T. Mora, Beatriz Trenor.

**Writing – review & editing:** Maria T. Mora, Jose M. Ferrero, Lucia Romero, Beatriz Trenor.

## References

1. Drouin E, Lande G, Charpentier F. Amiodarone reduces transmural heterogeneity of repolarization in the human heart. *J Am Coll Cardiol.* 1998; 32: 1063–1067. [https://doi.org/10.1016/S0735-1097\(98\)00330-1](https://doi.org/10.1016/S0735-1097(98)00330-1) PMID: 9768733
2. Li G-R, Lau C-P, Leung T-K, Nattel S. Ionic current abnormalities associated with prolonged action potentials in cardiomyocytes from diseased human right ventricles. *Heart Rhythm.* 2004; 1: 460–468. <https://doi.org/10.1016/j.hrthm.2004.06.003> PMID: 15851200

3. Piacentino V, Weber CR, Chen X, Weisser-Thomas J, Margulies KB, Bers DM, et al. Cellular basis of abnormal calcium transients of failing human ventricular myocytes. *Circ Res*. 2003; 92: 651–658. <https://doi.org/10.1161/01.RES.0000062469.83985.9B> PMID: 12600875
4. Gomez JF, Cardona K, Trenor B. Lessons learned from multi-scale modeling of the failing heart. *J Mol Cell Cardiol*. 2015; 89: 146–159. <https://doi.org/10.1016/j.yjmcc.2015.10.016> PMID: 26476237
5. Beuckelmann DJ, Näbauer M, Krüger C, Erdmann E. Altered diastolic  $[Ca^{2+}]_i$  handling in human ventricular myocytes from patients with terminal heart failure. *Am Heart J*. 1995; 129: 684–689. [https://doi.org/10.1016/0002-8703\(95\)90316-X](https://doi.org/10.1016/0002-8703(95)90316-X) PMID: 7900618
6. Bers DM. Altered cardiac myocyte Ca regulation in heart failure. *Physiology*. 2006; 21: 380–387. <https://doi.org/10.1152/physiol.00019.2006> PMID: 17119150
7. Lou Q, Fedorov V V., Glukhov A V., Moazami N, Fast VG, Efimov IR. Transmural heterogeneity and remodeling of ventricular excitation-contraction coupling in human heart failure. *Circulation*. 2011; 123: 1881–1890. <https://doi.org/10.1161/CIRCULATIONAHA.110.989707> PMID: 21502574
8. Alpert NR, Hasenfuss G, Leavitt BJ, Littleman FP, Pieske B, Mulieri LA. A mechanistic analysis of reduced mechanical performance in human heart failure. *Jpn Hear J*. 2000; 41: 103–115.
9. Hasenfuss G, Meyer M, Schillinger W, Preuss M, Pieske B, Just H. Calcium handling proteins in the failing human heart. *Basic Res Cardiol*. 1997; 92 Suppl 1: 87–93. <https://doi.org/10.1007/BF00794072>
10. Houser SR, Piacentino V, Mattiello J, Weisser J, Gaughan JP. Functional properties of failing human ventricular myocytes. *Trends Cardiovasc Med*. 2000; 10: 101–7. [https://doi.org/10.1016/S1050-1738\(00\)00057-8](https://doi.org/10.1016/S1050-1738(00)00057-8) PMID: 11427996
11. Lou Q, Janardhan A, Efimov IR. Remodeling of calcium handling in human heart failure. *Adv Exp Med Biol*. 2012; 740: 1145–74. [https://doi.org/10.1007/978-94-007-2888-2\\_52](https://doi.org/10.1007/978-94-007-2888-2_52) PMID: 22453987
12. Zima A V., Bovo E, Mazurek SR, Rochira JA, Li W, Terentyev D. Ca handling during excitation-contraction coupling in heart failure. *Pflugers Arch Eur J Physiol*. 2014; 466: 1129–1137. <https://doi.org/10.1007/s00424-014-1469-3> PMID: 24515294
13. Gorski PA, Ceholski DK, Hajjar RJ. Altered myocardial calcium cycling and energetics in heart failure—A rational approach for disease treatment. *Cell Metab*. 2015; 21: 183–194. <https://doi.org/10.1016/j.cmet.2015.01.005> PMID: 25651173
14. Acsai K, Ördög B, Varró A, Nánási PP. Role of the dysfunctional ryanodine receptor— $Na^+$ - $Ca^{2+}$  exchanger axis in progression of cardiovascular diseases: What we can learn from pharmacological studies? *Eur J Pharmacol*. 2016; 779: 91–101. <https://doi.org/10.1016/j.ejphar.2016.03.016> PMID: 26970182
15. Roe AT, Frisk M, Louch WE. Targeting cardiomyocyte  $Ca^{2+}$  homeostasis in heart failure. *Curr Pharm Des*. 2015; 21: 431–48. <https://doi.org/10.2174/138161282104141204124129> PMID: 25483944
16. Romero L, Pueyo E, Fink M, Rodríguez B. Impact of ionic current variability on human ventricular cellular electrophysiology. *Am J Physiol Heart Circ Physiol*. 2009; 297: H1436–H1445. <https://doi.org/10.1152/ajpheart.00263.2009> PMID: 19648254
17. Trenor B, Cardona K, Gomez JF, Rajamani S, Ferrero JM, Belardinelli L, et al. Simulation and Mechanistic Investigation of the Arrhythmogenic Role of the Late Sodium Current in Human Heart Failure. *PLoS One*. 2012; 7: e32659. <https://doi.org/10.1371/journal.pone.0032659> PMID: 22427860
18. Cai L, Wang Y, Gao H, Li Y, Luo X. A mathematical model for active contraction in healthy and failing myocytes and left ventricles. *PLoS One*. 2017; 12: e0174834. <https://doi.org/10.1371/journal.pone.0174834> PMID: 28406991
19. O'Hara T, Virág L, Varró A, Rudy Y. Simulation of the undiseased human cardiac ventricular action potential: model formulation and experimental validation. *PLoS Comput Biol*. 2011; 7: e1002061. <https://doi.org/10.1371/journal.pcbi.1002061> PMID: 21637795
20. Passini E, Mincholé A, Coppini R, Cerbai E, Rodriguez B, Severi S, et al. Mechanisms of pro-arrhythmic abnormalities in ventricular repolarisation and anti-arrhythmic therapies in human hypertrophic cardiomyopathy. *J Mol Cell Cardiol*. 2016; 96: 72–81. <https://doi.org/10.1016/j.yjmcc.2015.09.003> PMID: 26385634
21. ten Tusscher KHWJ, Noble D, Noble PJ, Panfilov A V. A model for human ventricular tissue. *Am J Physiol Heart Circ Physiol*. 2004; 286: H1573–89. <https://doi.org/10.1152/ajpheart.00794.2003> PMID: 14656705
22. Maltsev VA, Undrovinas AI. A multi-modal composition of the late  $Na^+$  current in human ventricular cardiomyocytes. *Cardiovasc Res*. 2006; 69: 116–127. <https://doi.org/10.1016/j.cardiores.2005.08.015> PMID: 16223473
23. Gomez JF, Cardona K, Romero L, Ferrero JM, Trenor B. Electrophysiological and structural remodeling in heart failure modulate arrhythmogenesis. 1D simulation study. *PLoS One*. 2014; 9: e106602. <https://doi.org/10.1371/journal.pone.0106602> PMID: 25191998

24. Schmidt U, Hajjar RJ, Helm PA, Kim CS, Doye AA, Gwathmey JK. Contribution of Abnormal Sarcoplasmic Reticulum ATPase Activity to Systolic and Diastolic Dysfunction in Human Heart Failure. *J Mol Cell Cardiol.* 1998; 30: 1929–1937. <https://doi.org/10.1006/jmcc.1998.0748> PMID: 9799647
25. Lindner M, Erdmann E, Beuckelmann DJ. Calcium Content of the Sarcoplasmic Reticulum in Isolated Ventricular Myocytes from Patients with Terminal Heart Failure. *J Mol Cell Cardiol.* 1998; 30: 743–749. <https://doi.org/10.1006/jmcc.1997.0626> PMID: 9602423
26. Kubo H, Margulies KB, Piacentino V, Gaughan JP, Houser SR. Patients With End-Stage Congestive Heart Failure Treated With B-Adrenergic Receptor Antagonists Have Improved Ventricular Myocyte Calcium Regulatory Protein Abundance. *Circulation.* 2001; 104: 1012–1018. <https://doi.org/10.1161/hc3401.095073> PMID: 11524394
27. Njeim MT, Hajjar RJ. Gene therapy for heart failure. *Arch Cardiovasc Dis.* 2010; 103: 477–85. <https://doi.org/10.1016/j.acvd.2010.04.004> PMID: 21074127
28. Kho C, Lee A, Hajjar RJ. Altered sarcoplasmic reticulum calcium cycling—targets for heart failure therapy. *Nat Rev Cardiol.* 2012; 9: 717–33. <https://doi.org/10.1038/nrcardio.2012.145> PMID: 23090087
29. Bode EF, Briston SJ, Overend CL, O'Neill SC, Trafford AW, Eisner DA. Changes of SERCA activity have only modest effects on sarcoplasmic reticulum Ca<sup>2+</sup> content in rat ventricular myocytes. *J Physiol.* 2011; 589: 4723–9. <https://doi.org/10.1113/jphysiol.2011.211052> PMID: 21825024
30. Sankaranarayanan R, Li Y, Greensmith DJ, Eisner DA, Venetucci L. Biphasic decay of the Ca transient results from increased sarcoplasmic reticulum Ca leak. *J Physiol.* 2016; 594: 611–623. <https://doi.org/10.1113/JP271473> PMID: 26537441
31. Miller L, Greensmith DJ, Sankaranarayanan R, O'Neill SC, Eisner DA. The effect of 2,5-di-(tert-butyl)-1,4-benzohydroquinone (TBQ) on intracellular Ca<sup>2+</sup> handling in rat ventricular myocytes. *Cell Calcium.* 2015; 58: 208–214. <https://doi.org/10.1016/j.ceca.2015.05.002> PMID: 26120055
32. Teucher N, Prestle J, Seidler T, Currie S, Elliott EB, Reynolds DF, et al. Excessive sarcoplasmic/endo-plasmic reticulum Ca<sup>2+</sup>-ATPase expression causes increased sarcoplasmic reticulum Ca<sup>2+</sup> uptake but decreases myocyte shortening. *Circulation.* 2004; 110: 3553–3559. <https://doi.org/10.1161/01.CIR.0000145161.48545.B3> PMID: 15505097
33. Morimoto S, Hongo K, Kusakari Y, Komukai K, Kawai M, O-Uchi J, et al. Genetic modulation of the SERCA activity does not affect the Ca<sup>2+</sup> leak from the cardiac sarcoplasmic reticulum. *Cell Calcium.* 2014; 55: 17–23. <https://doi.org/10.1016/j.ceca.2013.10.005> PMID: 24290743
34. Lyon AR, Bannister ML, Collins T, Pearce E, Sepelripour AH, Dubb SS, et al. SERCA2a gene transfer decreases sarcoplasmic reticulum calcium leak and reduces ventricular arrhythmias in a model of chronic heart failure. *Circ Arrhythmia Electrophysiol.* 2011; 4: 362–372. <https://doi.org/10.1161/CIRCEP.110.961615> PMID: 21406682
35. del Monte F, Harding SE, Schmidt U, Matsui T, Kang ZB, Dec GW, et al. Restoration of contractile function in isolated cardiomyocytes from failing human hearts by gene transfer of SERCA2a. *Circulation.* 1999; 100: 2308–11. <https://doi.org/10.1161/01.CIR.100.23.2308> PMID: 10587333
36. Rocchetti M, Alemanni M, Mostacciolo G, Barassi P, Altomare C, Chisci R, et al. Modulation of Sarcoplasmic Reticulum Function by PST2744 [Istaroxime; (E,Z)-3-((2-Aminoethoxy)imino) Androstane-6,17-dione Hydrochloride]] in a Pressure-Overload Heart Failure Model. *J Pharmacol Exp Ther.* 2008; 326: 957–965. <https://doi.org/10.1124/jpet.108.138701> PMID: 18539651
37. Szentandrassy N, Birinyi P, Szigeti G, Farkas A, Magyar J, Tóth A, et al. SEA0400 fails to alter the magnitude of intracellular Ca<sup>2+</sup> transients and contractions in Langendorff-perfused guinea pig heart. *Nau-nyn Schmiedebergs Arch Pharmacol.* 2008; 378: 65–71. <https://doi.org/10.1007/s00210-008-0296-5> PMID: 18458877
38. Nagy ZA, Virág L, Tóth A, Biliczki P, Acsai K, Bányász T, et al. Selective inhibition of sodium-calcium exchanger by SEA-0400 decreases early and delayed after depolarization in canine heart. *Br J Pharmacol.* 2004; 143: 827–31. <https://doi.org/10.1038/sj.bjp.0706026> PMID: 15504749
39. Birinyi P, Tóth A, Jóna I, Acsai K, Almássy J, Nagy N, et al. The Na<sup>+</sup>/Ca<sup>2+</sup> exchange blocker SEA0400 fails to enhance cytosolic Ca<sup>2+</sup> transient and contractility in canine ventricular cardiomyocytes. *Cardio-vasc Res.* 2008; 78: 476–484. <https://doi.org/10.1093/cvr/cvn031> PMID: 18252759
40. Ozdemir S, Bito V, Holemans P, Vinet L, Mercadier JJ, Varro A, et al. Pharmacological inhibition of Na<sup>+</sup>/Ca exchange results in increased cellular Ca<sup>2+</sup> load attributable to the predominance of forward mode block. *Circ Res.* 2008; 102: 1398–1405. <https://doi.org/10.1161/CIRCRESAHA.108.173922> PMID: 18451338
41. Terracciano CMN, Philipson KD, MacLeod KT. Overexpression of the Na<sup>+</sup>/Ca<sup>2+</sup> exchanger and inhibition of the sarcoplasmic reticulum Ca<sup>2+</sup>-ATPase in ventricular myocytes from transgenic mice. *Cardio-vasc Res.* 2001; 49: 38–47. [https://doi.org/10.1016/S0008-6363\(00\)00205-4](https://doi.org/10.1016/S0008-6363(00)00205-4) PMID: 11121794
42. Wang J, Chan TO, Zhang X-Q, Gao E, Song J, Koch WJ, et al. Induced overexpression of Na<sup>+</sup>/Ca<sup>2+</sup> exchanger transgene: altered myocyte contractility, [Ca<sup>2+</sup>]<sub>i</sub> transients, SR Ca<sup>2+</sup> contents, and action

- potential duration. *Am J Physiol Hear Circ Physiol*. 2009; 297: H590–H601. <https://doi.org/10.1152/ajpheart.00190.2009> PMID: 19525383
43. Gandhi A, Siedlecka U, Shah AP, Navaratnarajah M, Yacoub MH, Terracciano CM. The effect of SN-6, a novel sodium-calcium exchange inhibitor, on contractility and calcium handling in isolated failing rat ventricular myocytes. *Cardiovasc Ther*. 2013; 31: 115–124. <https://doi.org/10.1111/1755-5922.12045>
  44. Shannon TR, Ginsburg KS, Bers DM. Quantitative assessment of the SR Ca<sup>2+</sup> leak-load relationship. *Circ Res*. 2002; 91: 594–600. <https://doi.org/10.1161/01.RES.0000036914.12686.28> PMID: 12364387
  45. Greensmith DJ, Galli GLJ, Trafford AW, Eisner DA. Direct measurements of SR free Ca reveal the mechanism underlying the transient effects of RyR potentiation under physiological conditions. *Cardiovasc Res*. 2014; 103: 554–563. <https://doi.org/10.1093/cvr/cvu158> PMID: 24947416
  46. Sobie EA. Parameter sensitivity analysis in electrophysiological models using multivariable regression. *Biophys J*. 2009; 96: 1264–1274. <https://doi.org/10.1016/j.bpj.2008.10.056> PMID: 19217846
  47. Walmsley J, Rodriguez JF, Mirams GR, Burrage K, Efimov IR, Rodriguez B. mRNA Expression Levels in Failing Human Hearts Predict Cellular Electrophysiological Remodeling: A Population-Based Simulation Study. *PLoS One*. 2013; 8: e56359. <https://doi.org/10.1371/journal.pone.0056359> PMID: 23437117
  48. Jost N, Virág L, Comtois P, Ordög B, Szuts V, Seprényi G, et al. Ionic mechanisms limiting cardiac repolarization reserve in humans compared to dogs. *J Physiol*. 2013; 591: 4189–206. <https://doi.org/10.1113/jphysiol.2013.261198> PMID: 23878377
  49. Valdivia CR, Chu WW, Pu J, Foell JD, Haworth RA, Wolff MR, et al. Increased late sodium current in myocytes from a canine heart failure model and from failing human heart. *J Mol Cell Cardiol*. 2005; 38: 475–483. <https://doi.org/10.1016/j.yjmcc.2004.12.012> PMID: 15733907
  50. Undrovinas AI, Belardinelli L, Undrovinas NA, Sabbah HN. Ranolazine improves abnormal repolarization and contraction in left ventricular myocytes of dogs with heart failure by inhibiting late sodium current. *J Cardiovasc Electrophysiol*. 2006; 17: S169–S177. <https://doi.org/10.1111/j.1540-8167.2006.00401.x> PMID: 16686675
  51. Levi AJ, Dalton GR, Hancox JC, Mitcheson JS, Issberner J, Bates JA, et al. Role of intracellular sodium overload in the genesis of cardiac arrhythmias. *J Cardiovasc Electrophysiol*. 1997; 8: 700–721. PMID: 9209972
  52. Pieske B, Maier LS, Piacentino V, Weisser J, Hasenfuss G, Houser S. Rate dependence of [Na<sup>+</sup>]<sub>i</sub> and contractility in nonfailing and failing human myocardium. *Circulation*. 2002; 106: 447–453. <https://doi.org/10.1161/01.CIR.0000023042.50192.F4> PMID: 12135944
  53. Bueno-rovio A, Sánchez C, Pueyo E. Na/K pump regulation of cardiac repolarization: insights from a systems biology approach. *Pflugers Arch Eur J Physiol*. 2014; 466: 183–193. <https://doi.org/10.1007/s00424-013-1293-1> PMID: 23674099
  54. Shannon TR, Wang F, Puglisi J, Weber C, Bers DM. A Mathematical Treatment of Integrated Ca Dynamics within the Ventricular Myocyte. *Biophys J*. 2004; 87: 3351–3371. <https://doi.org/10.1529/biophysj.104.047449> PMID: 15347581
  55. Grandi E, Pasqualini FS, Bers DM. A novel computational model of the human ventricular action potential and Ca transient. *J Mol Cell Cardiol*. 2010; 48: 112–121. <https://doi.org/10.1016/j.yjmcc.2009.09.019> PMID: 19835882
  56. Priebe L, Beuckelmann DJ. Simulation study of cellular electric properties in heart failure. *Circ Res*. 1998; 82: 1206–1223. <https://doi.org/10.1161/01.RES.82.11.1206> PMID: 9633920
  57. Zhang Yu, Shou Guofa, Xia Ling. Simulation Study of Transmural Cellular Electrical Properties in Failed Human Heart. *Conf Proc IEEE Eng Med Biol*. 2005. pp. 337–340. <https://doi.org/10.1109/IEMBS.2005.1616413> PMID: 17282182
  58. Elshrif MM, Shi P, Cherry EM. Representing Variability and Transmural Differences in a Model of Human Heart Failure. *IEEE J Biomed Heal Informatics*. 2015; 19: 1308–1320. <https://doi.org/10.1109/JBHI.2015.2442833> PMID: 26068919